ELSEVIER

Polymer 43 (2002) 3007–3017

polymer

www.elsevier.com/locate/polymer

Synthesis and characterization of polyethylene-like polyurethanes derived from long-chain, aliphatic α,ω-diols

Robin L. McKiernan, Samuel P. Gido, Jacques Penelle*

Department of Polymer Science and Engineering, University of Massachusetts, Amherst, MA 01003-4530, USA

Received 4 October 2001; received in revised form 22 January 2002; accepted 24 January 2002

Abstract

Long-chain aliphatic α,ω-diols containing up to 32 consecutive methylene groups were synthesized by several methods and characterized. 1,22-Docosanediol HO–$(CH_2)_{22}$–OH and 1,32-dotriacontanediol HO–$(CH_2)_{32}$–OH both exhibited a solid–solid phase transition before melting. The α,ω-diols HO–$(CH_2)_m$–OH, where $m = 12$, 22, or 32, were reacted in the melt with much shorter aliphatic α,ω-diisocyanates O=C=N–$(CH_2)_n$–N=C=O, where $n = 4$, 6, 8, or 12, producing a series of linear, aliphatic, and increasingly polyethylene-like *m*,*n*-polyurethanes. Characterization (by DSC, TGA, and SAXS) of the *m*,*n*-polyurethane series showed that when the aliphatic segments were increased, and the hydrogen-bonding densities thus decreased, the polymers displayed physical and thermal properties (for example, solubility and melting temperature) typical of polyethylene. © 2002 Elsevier Science Ltd. All rights reserved.

Keywords: Long-chain α,ω-diols; Hydrogen-bonding; Linear *m*,*n*-polyurethanes

1. Introduction

It is well known that the introduction of hydrogen-bonding units (e.g. amide –C(O)–NH– or urethane –O–C(O)–NH–) on an otherwise purely aliphatic polymer dramatically influences the way the macromolecule will crystallize [1]. The crystallization of polyethylene is controlled by van der Waals forces resulting in the orthorhombic packing of the all *trans* chains with the crystal planes oriented perpendicular to each other (Fig. 1(a)). On the contrary, the introduction of hydrogen-bonds to the backbone in polymers, such as in polyamides and polyurethanes, results in either triclinic or monoclinic packing (as well as a varying amount of pseudo-hexagonal packing) with the crystal planes oriented parallel to each other in order to maximize the contribution of the hydrogen-bonds between neighboring stems (Fig. 1(b)) [2–6]. Hydrogen bonds alter not only the crystal structure of an otherwise aliphatic polymer, but also the polymer's morphology, crystallization kinetics, and resulting thermal properties.

The primary purpose of this study is to chemically engineer the crystallinity of a series of semi-crystalline polymers by introducing urethane –O–C(O)–NH– units capable of undergoing hydrogen-bonding in a well-controlled manner onto a poly(*m*)ethylene chain $(CH_2)_m$ or $(CH_2–CH_2)_m$. Model, long-chain, aliphatic polyurethanes of the general structure –[O–$(CH_2)_m$–O–C(O)–NH–$(CH_2)_n$–NH–C(O)$]_x$– were synthesized for the previously stated purpose. By progressively increasing the length of the aliphatic α,ω-diols HO–$(CH_2)_m$–OH used as monomers, the hydrogen-bonding density of the polyurethanes was diluted, resulting in a series of polymers that bridged the gap in the spectrum from polyethylene to polymers capable of forming hydrogen-bonds, such as polyamides and polyurethanes. This paper focuses on the synthesis of these long-chain, hydrogen-bonded polymers, as well as their thermal and physical properties, and is the first in a series on the morphology and crystallization kinetics [7–9].

Very long-chain, aliphatic polyurethanes have not been investigated in the past in part due to the lack of pure, long chain α,ω-monomers. The longest purely aliphatic polyurethane previously synthesized is the 16,10-polyurethane by Saotome and Komoto [10]. They examined the influence of increasing aliphatic length on the thermal properties of a series of *m*,*n*-polyurethanes and polyureas. There has recently been research into the synthesis of other long-chain polymers such as biodegradable 30,30-polyester [11] and polyamide–polyolefin blend compatibilizers 6,24- and 6,34-polyamides [12]. In this study, long-chain aliphatic diols of up to 32 consecutive methylene groups were used to synthesize these long-chain, model polymers. The synthesis of these α,ω-diols was accomplished via modified literature procedures including the coupling of

---

* Corresponding author. Fax: +1-413-545-0082.
E-mail address: penelle@mail.pse.umass.edu (J. Penelle).

PII: S0032-3861(02)00096-4

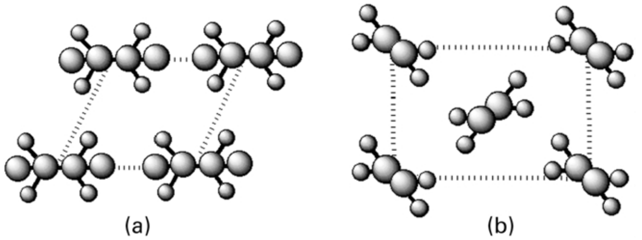

Fig. 1. Crystal structure typical of (a) polyurethane/polyamide and (b) polyethylene.

either halogenated alcohols or enamines. Due to the versatility of these synthetic methods, the synthesis of numerous other longer aliphatic α,ω-diols is possible, and their synthesis is currently underway.

2. Experimental

2.1. Characterization

^{1}H and ^{13}C NMR spectra of the monomers and polymers were obtained either in deuterated chloroform or benzene from a Bruker 300 MHz nuclear magnetic resonance (NMR) spectrometer at room temperature or in deuterated chloroform, dimethylsulfoxide (DMSO), or dimethylformamide (DMF) from a Bruker 500 or 600 MHz spectrometer at elevated temperatures. Infrared spectra were recorded on a Bio-Rad FTS 175C spectrometer using 16 scans. Elemental analysis was carried out by the Microanalytical Laboratory of the University of Massachusetts, Amherst via the classical Modified Pregl–Dumas reaction using an Exeter Analytical 240A elemental analyzer. Absolute molecular weights and distributions of the polymers were determined by high temperature, triple detector gel permeation chromatography (GPC). A Polymer Laboratory PL-GPC 220 ultra high temperature chromatograph with a Hewlett-Packard 1100 series isocratic pump was employed with PL gel 20 μm mixed-A columns. The system was equipped with a Polymer Labs differential refractive index detector, Viscotek viscometer and Wyatt Technology heated miniDAWN light scattering detector that used a wavelength of 690 nm. Instrument constants were determined using 200 000 molecular weight polystyrene. Wyatt Technology's ASTRA software (version 4.70) was used to work out the data. All of the GPC experiments were performed using 1,2,4-trichlorobenzene as the mobile phase at 135 °C.

2.2. Thermal analysis

Thermogravimetric analysis (TGA) was performed on the monomers and polymers (5–10 mg) using a TA Instruments TGA 2950 flushed with nitrogen at a scan rate of 10 K min^{-1}. Decomposition temperatures were taken at 5% weight loss. Melting points were observed using either a Perkin Elmer Pyris or TA Instruments Universal V2.5H differential scanning calorimeter (DSC) flushed with helium. The samples (5–10 mg) were heated above their melting points to 200 °C, cooled to room temperature, and then reheated, all at a rate of 10 K min^{-1}. The melting points were taken as the peak of the melting endotherm during the second heating run. The temperature scale was calibrated using indium and eicosane, and the heat of enthalpy was calibrated using indium.

2.3. Monomer and polymer synthesis

All of the diisocyanates were commercially available and distilled immediately before use. 1,12-Dodecanediol HO–$(CH_2)_{12}$–OH was also commercially available. 1,22-Docosanediol and 1,32-dotriacontanediol were synthesized using modified literature procedures (described later). All of the α,ω-diols (commercial and synthesized) were dried in a vacuum oven to remove absorbed water. Reagents used during the synthesis of these diols were obtained commercially, and unless otherwise stated they were used without further purification. Triethylamine was dried over calcium hydride. Cyclohexane and chloroform were dried using phosphorous pentoxide. Acetone was dried with potassium carbonate. Tetrahydrofuran (THF) was dried over sodium and benzophenone. The Wurtz coupling reaction was performed using a VCX 600 ultrasonicator at 30% amplitude.

2.3.1. 11-Bromo-1-(trimethylsilyloxy)undecane (1)

Under an argon atmosphere, 11-bromo-1-undecanol (53.91 g, 0.21 mol) was dissolved in triethylamine (210 ml) at room temperature. Trimethylchlorosilane (25.68 g, 0.24 mol) was added dropwise to the rapidly stirred light brown solution, and a white solid formed immediately. After 3.5 h, petroleum ether (200 ml) was added to the mixture. The mixture was then filtered and washed with additional petroleum ether (500 ml). The transparent yellow solution was evaporated yielding 11-bromo-1-(trimethylsilyloxy)undecane (**1**) as a white powder (49.30 g, 71%). ^{1}H NMR (300 MHz, $CDCl_3$) δ 3.56 (t, $J = 6.8$ Hz, 2H, CH_2–OTMS), 3.40 (t, $J = 6.8$ Hz, 2H, CH_2–Br), 1.85 (p, $J = 6.8$ Hz, 2H, CH_2–CH_2–Br), 1.52 (p, $J = 6.8$ Hz, 2H, CH_2–CH_2–OTMS), 1.50–1.20 (m, 14H, CH_2–CH_2–CH_2), 0.11 (s, 9H, OSi–(CH_3)$_3$).

2.3.2. 11-Iodo-1-(trimethylsilyloxy)undecane (2)

11-Bromo-1-(trimethylsilyloxy)undecane (**1**) (46.29 g, 0.14 mol), sodium iodide (37.48 g, 0.25 mol), and acetone (205 ml) were mixed together and then refluxed for 2 h. The resulting yellow solution was evaporated. Petroleum ether was then added, and the mixture was filtered and washed with more petroleum ether (500 ml). Evaporation of the solvent yielded 11-iodo-1-(trimethylsilyloxy)undecane (**2**) (46.08 g, 87%) as a light yellow solution. ^{1}H NMR (300 MHz, $CDCl_3$) δ 3.57 (t, $J = 6.8$ Hz, 2H, CH_2–OTMS), 3.19 (t, $J = 7.2$ Hz, 2H, CH_2–I), 1.82 (p, $J = 7.2$ Hz, 2H, CH_2–CH_2–I), 1.53 (p, $J = 6.8$ Hz, 2H, CH_2–CH_2–OTMS), 1.40–1.25 (m, 14H, CH_2–CH_2–CH_2), 0.11 (s, 9H, OSi–(CH_3)$_3$).

2.3.3. *1,22-Docosanediol (**3**)*

Finely cut pieces of sodium (1.19 g, 51.76 mmol) were added to cyclohexane (28.5 ml) in an argon-purged double-jacketed four-necked glass vessel. The mixture was pre-sonicated at 30% amplitude for 30 min, during which time the mixture turned a slight gray. Cold water was circulated through the jacket of the vessel to cool the mixture. 11-Iodo-1-(trimethylsilyloxy)undecane (**2**) (10.55 g, 28.48 mmol) was added, and the mixture immediately turned a deep opaque blue. The homogeneous mixture was then sonicated for another 3.5 h. After cooling to room temperature, methanol (14 ml) was slowly added to decompose any remaining sodium, and a white solid immediately appeared. The mixture was then carefully treated with deionized water (2.5 ml) and sulfuric acid (1 mol l^{-1}, 10 ml). The product was filtered and washed with deionized water (70 ml) up to neutrality. The resulting white solid was recrystallized from methanol (215 ml) to yield pure 1,22-docosanediol (**3**) (2.89 g, 59%); mp 106.8 °C, lit.: 106–107 °C [13], 103.1 °C [14], 106 °C [15]. ^{1}H NMR (300 MHz, $CDCl_3$) δ 3.65 (q, $J = 6.6$ Hz, 4H, CH_2–OH), 1.58 (m, 4H, CH_2–CH_2–OH), 1.40–1.20 (m, 36H, CH_2–CH_2–CH_2). ^{13}C NMR (500 MHz, $CDCl_3$, 323 K) δ 63.36 (CH$_2$OH), 33.15 (CH$_2$CH$_2$OH), 29.92, 29.91, 29.90, 29.86, 29.84, 29.69 (all aliphatic CH$_2$), 26.03 (CH$_2$CH$_2$CH$_2$OH). IR (KBr): 3304 cm^{-1} (OH stretch), 2918 cm^{-1} (asymmetric CH stretch), 2849 cm^{-1} (symmetric CH stretch), 1474 and 1462 cm^{-1} (CH_2 bend), 731 cm^{-1} (in-phase CH_2 rock), 719 cm^{-1} (out-of-phase CH_2 rock). Anal. calcd for $C_{22}H_{46}O_2 \cdot (H_2O)_{2.1}$ (344.5): C, 76.68; H, 13.52. Found: C, 76.62; H, 13.83.

2.3.4. *1-Morpholino-1-cyclododecene (**4**)*

Cyclododecanone (30.50 g, 0.17 mol), morpholine (29.05 g, 0.33 mol), benzene (75 ml), and *p*-toluenesulfonic acid (*p*-TSOH, trace amounts) were added to a two-necked flask equipped with a Dean–Stark trap. The mixture was refluxed until no additional water was collected in the trap (2–3 days). Benzene and any excess morpholine were then evaporated off. Cyclododecanone, a white solid, was distilled with the aid of a heat gun to keep the cyclododecanone from solidifying in the distillation apparatus. Distillation of the remaining brown liquid resulted in isolating 1-morpholino-1-cyclododecene (**4**) as a clear liquid (33.99 g, 81%). ^{1}H NMR (300 MHz, $CDCl_3$) δ 4.20 (t, $J = 7.7$ Hz, 1H, CH=CR), 3.42 (t, $J = 4.7$ Hz, 4H, CH_2–O), 2.40 (t, $J = 4.7$ Hz, 4H, CH_2–N), 2.00 (m, 4H, CH_2–CH=CR), 1.40–1.20 (m, 20H, CH_2–CH_2–CH_2).

2.3.5. *1,4-Bis-(2,14-dioxo-cyclotetradecyl)-butane (**5**)*

1-Morpholino-1-cyclododecene (**4**) (4.94 g, 19.64 mmol), chloroform (2.5 ml), and triethylamine (3 ml) were added to a three-necked flask under argon and cooled in an ice/water/salt bath. Suberoyl chloride (1.58 g, 7.50 mmol) in chloroform (2.5 ml) was slowly added dropwise while keeping the temperature of the mixture below 15 °C. After addition of the acid, the yellow mixture was allowed to warm to room temperature and stirred for 4 h. Chloroform (40 ml) and hydrochloric acid (2.5 mol l^{-1}, 20 ml) were added, and the mixture was stirred for 24 h. The two phases were then separated. The aqueous layer was extracted with chloroform (6 × 5 ml aliquots) and the organic phase with deionized water (6 × 5 ml aliquots). The chloroform from the combined organic phases was evaporated. The resulting yellow solid was recrystallized from ethyl acetate (100 ml) yielding 1,4-bis-(2,14-dioxo-cyclotetradecyl)-butane (**5**) as a white powder (1.05 g, 28%); mp 187.3 °C, lit.: 183–184 °C [16]. ^{1}H NMR (300 MHz, $CDCl_3$) δ 3.57 (t, $J = 7.2$ Hz, 2H, CH–(C=O)$_2$), 2.50–2.30 (m, 8H, CH_2–(C=O)), 1.80–1.50 (m, 12H, CH_2–CHR–(C=O)), 1.40–1.10 (m, 26H, CH_2–CH_2–CH_2).

2.3.6. *13,20-Dioxo-dotriacontanedioic acid (**6**)*

Sodium hydroxide (5.80 g, 0.15 mol) and 1,4-bis-(2,14-dioxo-cyclotetradecyl)-butane (**5**) (11.21 g, 22.29 mmol) were each separately refluxed in 2-methoxyethanol (65 and 110 ml, respectively) until they dissolved. The two red solutions were then combined, and a white solid quickly formed. After refluxing the combined mixture for 1.5 h, the mixture was filtered and washed first with 2-methoxyethanol and then ethanol. The resulting pink solid was recrystallized from acetic acid (400 ml) to yield 13,20-dioxo-dotriacontanedioic acid (**6**) as a white powder (11.75 g, 99%); mp 145.9 °C, lit.: 142 °C [16]. ^{1}H NMR (500 MHz, DMSO-d_6, 373 K) δ 2.37 (t, $J = 7.3$ Hz, 8H, CH_2–(C=O)), 2.19 (t, $J = 7.3$ Hz, 4H, CH_2–COOH), 1.54–1.48 (m, 12H, CH_2–CH_2–(C=O)), 1.25–1.32 (m, 32H, CH_2–CH_2–CH_2).

2.3.7. *1,32-Dotriacontanedioic acid (**7**)*

13,20-Dioxo-dotriacontanedioic acid (**6**) (3.83 g, 71.07 mmol), hydrazine hydrate (85%, 10 ml), and triethanolamine (32 ml) were added to a three-necked flask fitted with a condenser and thermometer. The mixture was heated at 125 °C for 2 h. Potassium hydroxide (2.15 g, 38.32 mmol) in triethanolamine (11.5 ml) was heated at 160 °C until the potassium hydroxide dissolved. Both mixtures were cooled to around 80 °C, and the potassium hydroxide solution was then carefully added to the hydrazone solution. The temperature of the solution was increased to 135 °C at which point foaming occurred. The solution was stirred at this temperature for 0.5 h. The condenser was then removed, and the temperature was increased to 195 °C over 1.5 h in order to drive off the water. Care is needed when raising the temperature in order to avoid excessive foaming. The reaction was stirred at 195 °C for 6.5 h. After cooling to room temperature, deionized water (60 ml) was added to the white solid. The temperature was raised to 100 °C and filtered hot. The sample was then recrystallized from acetic acid (150 ml) yielding 1,32-dotriacontanedioic (**7**) acid as a white solid (3.19 g, 88%); mp 129.3 °C, lit.: 128 °C [16]. ^{1}H NMR (500 MHz, DMSO-d_6, 373 K) δ 2.20 (t, $J = 7.2$ Hz, 4H, $\mathrm{C}H_2$–COOH), 1.57 (p, $J = 6.7$ Hz, 4H, $\mathrm{C}H_2$–$\mathrm{CH_2}$–COOH), 1.36–1.26 (m, 52H, $\mathrm{CH_2}$–$\mathrm{C}H_2$–$\mathrm{CH_2}$).

2.3.8. Dimethyl 1,32-dotriacontanoate (8)

1,32-Dotriacontanedioic acid (**7**) (6.38 g, 12.49 mmol), methanol (120 ml), and concentrated sulfuric acid (4.5 ml) were combined and refluxed for 16 h. After cooling, the mixture was filtered and washed with deionized water. The white powder was then recrystallized from methanol (50 ml) yielding dimethyl 1,32-dotriacontanoate (**8**) (6.48 g, 96%); mp 90.3 °C, lit.: 87–89 °C [17], 85.5–87 °C [18]. ^{1}H NMR (300 MHz, C_6D_6) δ 3.46 (s, 6H, $\mathrm{C}H_3$–O–(C=O)), 2.23 (t, $J = 7.3$ Hz, 4H, $\mathrm{C}H_2$–(C=O)), 1.68 (p, $J = 6.4$ Hz, 4H, $\mathrm{C}H_2$–$\mathrm{CH_2}$–(C=O)), 1.50–1.30 (m, 52H, $\mathrm{CH_2}$–$\mathrm{C}H_2$–$\mathrm{CH_2}$).

2.3.9. 1,32-Dotriacontanediol (9)

Dimethyl 1,32-dotriacontanoate (**8**) (0.98 g, 1.82 mmol) was added to THF (200 ml) and refluxed. Lithium aluminum hydride was carefully added to the refluxing solution in three portions over the course of a day (total 0.57 g, 15.02 mmol). The mixture was then refluxed for an additional day. After cooling the gray mixture, deionized water was carefully added until there was no more evolution of hydrogen gas. Concentrated hydrochloric acid was then added to the white mixture until a pH of 2 was reached. The mixture was filtered, and the white sample was recrystallized from a mixture (1:1 volume ratio) of methanol (50 ml) and chloroform (50 ml) to yield pure 1,32-dotriacontanediol (**9**) (0.57 g, 62%); mp 114.9 °C, lit.: 115–117 °C [18], 94 °C [19], 98 °C [20]. ^{1}H NMR (600 MHz, DMSO-d_6, 373 K) δ 3.42 (t, $J = 6.5$ Hz, 4H, $\mathrm{C}H_2$–OH), 1.45 (p, $J = 6.5$ Hz, 4H, $\mathrm{C}H_2$–$\mathrm{CH_2}$–OH), 1.42–1.26 (m, 56H, $\mathrm{CH_2}$–$\mathrm{C}H_2$–$\mathrm{CH_2}$). ^{13}C NMR (500 MHz, DMSO-d_6, 373 K) δ 60.36 ($C\mathrm{H_2OH}$), 31.96 ($C\mathrm{H_2CH_2OH}$), 28.37, 28.30, 28.27, 28.24 (all aliphatic $C\mathrm{H_2}$), 24.89 ($C\mathrm{H_2CH_2CH_2OH}$). IR (KBr): 3318 cm^{-1} (OH stretch), 2918 cm^{-1} (asymmetric CH stretch), 2849 cm^{-1} (symmetric CH stretch), 1472 and 1463 cm^{-1} ($\mathrm{CH_2}$ bend), 732 cm^{-1} (in-phase $\mathrm{CH_2}$ rock), 720 cm^{-1} (out-of-phase $\mathrm{CH_2}$ rock). Anal. calcd for $C_{32}H_{66}O_2{\cdot}(H_2O)_{21.1}$ (490.91): C, 77.33; H, 13.70. Found: C, 77.36; H, 13.69.

2.3.10. m,n-Polyurethanes

The diols (0.5 g) were heated above their melting temperatures in argon-purged glass vessels. Stoichiometric amounts of diisocyanates were syringed into the reaction vessels, and the mixtures were vigorously stirred for up to an hour or until they solidified. After cooling to room temperature, DMF (10 ml) was added, and the mixtures were heated until the polymers dissolved. The hot solutions were then poured dropwise into rapidly stirred methanol (100 ml). The resulting cloudy white mixtures were filtered and dried in a vacuum oven yielding *m*,*n*-polyurethanes $-[\mathrm{O}-(\mathrm{CH_2})_m-\mathrm{O}-\mathrm{C(O)}-\mathrm{NH}-(\mathrm{CH_2})_n-\mathrm{NH}-\mathrm{C(O)}]_x-$ as white solids. ^{1}H NMR (500 MHz, DMSO-d_6, 393–413 K) δ 6.37–6.27 (bs, 2H, NH), 3.96 (t, $J = 6.5$ Hz, 4H, $\mathrm{C}H_2$–O–C(O)), 3.16–3.00 (m, 4H, $\mathrm{C}H_2$–NH–C(O)), 1.57 (p, $J = 6.3$ Hz, 4H, $\mathrm{C}H_2$–$\mathrm{CH_2}$–O–C(O)), 1.45 (m, 4H, $\mathrm{C}H_2$–$\mathrm{CH_2}$–NH–C(O)), 1.30 (m, $\mathrm{CH_2}$–$\mathrm{C}H_2$–$\mathrm{CH_2}$). ^{1}H NMR (500 MHz, DMF-d_7, 393–413 K) δ 6.22–5.72 (bs, 2H, NH), 4.04–4.01 (t, $J = 6.5$ Hz, 4H, $\mathrm{C}H_2$–O–C(O)), 3.14–3.10 (m, 4H, $\mathrm{C}H_2$–NH–C(O)), 1.64–1.59 (p, $J = 6.3$ Hz, 4H, $\mathrm{C}H_2$–$\mathrm{CH_2}$–O–C(O)), 1.57–1.54 (m, 4H, $\mathrm{C}H_2$–$\mathrm{CH_2}$–NH–C(O)), 1.36–1.33 (m, $\mathrm{CH_2}$–$\mathrm{C}H_2$–$\mathrm{CH_2}$). ^{13}C NMR (500 MHz, DMSO-d_6, 393–413 K) δ 155.88–155.84 (O–C(O)–NH), 63.25–63.18 ($C\mathrm{H_2}$–O–C(O)–NH), 29.00–24.88 (remaining $C\mathrm{H_2}$). ^{13}C NMR (500 MHz, DMF-d_7, 393–413 K) δ 162.49–162.44 (O–C(O)–NH), 69.82–69.72 ($C\mathrm{H_2}$–O–C(O)–NH), 46.73–46.41 ($C\mathrm{H_2}$–NH–C(O)–O), 34.33–31.46 (remaining $C\mathrm{H_2}$). IR (KBr): 3333–3310 cm^{-1} (NH stretch), 2922–2918 cm^{-1} (asymmetric CH stretch), 2852–2849 cm^{-1} (symmetric CH stretch), 1696–1682 cm^{-1} (amide I), 1540–1537 cm^{-1} (amide II), 1475–1468 cm^{-1} ($\mathrm{CH_2}$ bend).

3. Results and discussions

3.1. Monomer synthesis

1,22-Docosanediol (**3**) $\mathrm{HO}-(\mathrm{CH_2})_{22}-\mathrm{OH}$ is a natural product found in potato tuber skin [21], stem bark and wood [22], cork [23], apple wax [24], and carnauba wax [25]. However, the purity of the diol is low and removal of the contaminants, typically other α,ω-diols or -diacids, is extremely difficult. A procedure developed by Rusanova et al. [13] and modified by Le Fevere de Ten Hove [26] was used to synthesize the diol (Scheme 1). Due to differences in sonication equipment, the final step (Wurtz reaction in the presence of metallic sodium) was again modified and optimized (Table 1). Using this method, commercially available 11-bromo-1-undecanol $\mathrm{Br}-(\mathrm{CH_2})_{11}-\mathrm{OH}$ was converted to the hydroxyl-protected trimethylsilyl ether (**1**) $\mathrm{Br}-(\mathrm{CH_2})_{11}-\mathrm{OSiMe_3}$. The bromine was replaced with the more reactive iodine via the Finkelstein reaction forming the protected iodo-alcohol (**2**) $\mathrm{I}-(\mathrm{CH_2})_{11}-\mathrm{OSiMe_3}$. Two

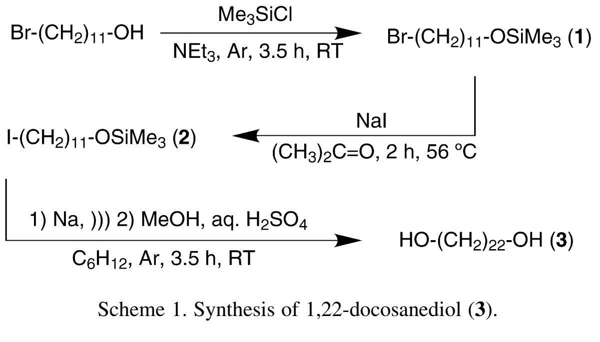

Scheme 1. Synthesis of 1,22-docosanediol (**3**).

Table 1
Optimization of the Wurtz coupling reaction

Solvent	Iodo-alcohol (mol)	Na (mol)	Heat/cool	Pre-sonicate (h)	Pulse	Time (h)	Yield (%)
Benzene[a]	0.2	0.35	Heat	0.5	No	18	58
Benzene	0.03	0.05	Heat	No	No	6	21
Benzene	0.03	0.05	Cool	No	No	3	48
Cyclohexane	0.03	0.05	Cool	No	No	4	38
Cyclohexane	0.03	0.05	Cool	No	2.5 s	5.5	35
Cyclohexane	0.03	0.03	Cool	0.5	No	4	36
Cyclohexane	0.03	0.05	Cool	0.5	No	3.5	55
Cyclohexane	0.03	0.05	Cool	0.5	No	3.5	59

[a] See Ref. [25].

equivalents of the protected iodo-alcohol were coupled using a sonically activated Wurtz coupling reaction and then deprotected to yield 1,22-docosanediol (**3**). The side product, 1-undecanol, was removed via recrystallization of the product followed by filtration. The global yield of the diol was 36%.

1,32-Dotriacontanediol (**9**) HO–$(CH_2)_{32}$–OH is also a natural product found in carnauba wax [27]. The diol was synthesized by the reduction of the corresponding diacid obtained from the enamine-coupling route developed by Hünig et al. [16] (Scheme 2). The enamine (**4**) was synthesized by the acid-catalyzed condensation of commercially available morpholine and cyclododecanone. A [2 + 2] cycloaddition of the enamine and suberoyl chloride Cl–C(O)–$(CH_2)_6$–C(O)–Cl produced the cyclic tetraketone (**5**), which was ring-opened under basic conditions to the dioxo-dioic acid (**6**) HO_2C–$(CH_2)_{11}$–C(O)–$(CH_2)_6$–C(O)–$(CH_2)_{11}$–CO_2H and then reduced via a Wolff–Kishner reaction to form the diacid (**7**) HO_2C–$(CH_2)_{30}$–CO_2H. The diacid was converted to the diester (**8**) H_3CO_2C–$(CH_2)_{30}$–CO_2CH_3 via an acid-catalyzed esterification, in order to increase its solubility in THF, and then reduced using lithium aluminum hydride to yield 1,32-dotriacontanediol (**9**). The global yield of the diol was 12%.

3.2. Monomer characterization and thermal properties

The ^1H and ^{13}C NMR spectra of the 1,22-docosanediol and 1,32-dotriacontanediol were fully compatible with the expected structures. After recrystallization of the diols, the side products, 1-undecanol and unreduced carbonyl groups, respectively, were not detectable. The infrared of

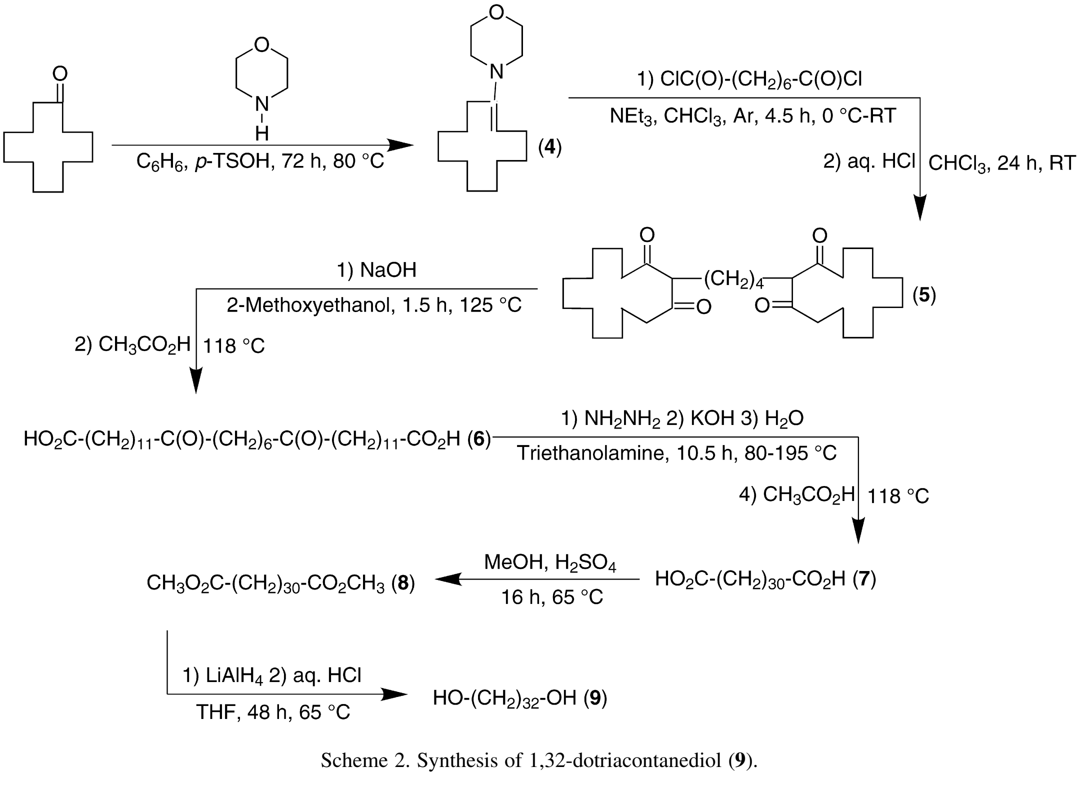

Scheme 2. Synthesis of 1,32-dotriacontanediol (**9**).

Table 2
Thermal properties of the α,ω-diols

α,ω-Diol	Melting temperature (°C)	Transition temperature[a] (°C)	Enthalpy (J g^{-1})	Decomposition temperature[b] (°C)
1,13[c]	78	70	217	
1,14[c]	87	No[d]	269	
1,15[c]	88	76	241	
1,16[c]	92	90	248	
1,17[c]	94	81	242	
1,18[c]	98	93	251	
1,19[c]	101	86	243	
1,20[c]	103	95	245	
1,21[c]	104	87	247	
1,22[c]	106	97	254	
1,23[c]	108	93	250	
1,24[c]	108	100	254	
1,44[e]	116	No[d]	273	
1,12	84	No[d]	264	182
1,22	107	97	268	235
1,32	115	99	240	292

[a] Melting temperatures were taken as the peak of the melting endotherm during the second heating run using a scan rate of 10 K min^{-1}.
[b] Decomposition temperatures were taken at 5% weight loss using a scan rate of 10 K min^{-1}.
[c] See Ref. [14].
[d] Indicates that no solid–solid phase transition was observed.
[e] See Ref. [25].

the 1,32-dotriacontanediol also indicated the absence of unreduced carbonyl groups. The infrared spectra of both diols showed the Davydov splittings typically seen for monoclinically or orthorhombically packed *n*-paraffins [28]. Elemental analysis results indicated that the diols were very hygroscopic as expected.

The thermal properties of the α,ω-diols are listed in Table 2. The aliphatic diols exhibited increasing decomposition and melting temperatures with increasing chain length (Fig. 2). 1,22-Docosanediol and 1,32-dotriacontanediol both showed solid–solid phase transitions upon both heating and cooling (Fig. 3). Ogawa and Nakamura previously showed that α,ω-alkanediols HO–$(CH_2)_n$–OH, with $n = 13$–24 (except for $n = 14$), undergo a reversible solid–solid phase transition [15]. Recently, Le Fevere de Ten Hove [26] showed that 1,44-tetratetracontanediol HO–$(CH_2)_{44}$–OH also exhibited a solid–solid phase transition upon cooling from the melt. A closer examination of 1,16-hexadecanediol HO–$(CH_2)_{16}$–OH by Kobayashi and Nakamura and 1,22-docosanediol by Le Fevere de Ten Hove et al. proved that this transition is a rotator phase transition [26,29]. This current study confirmed the absence of this transition for 1,12-dodecanediol and the existence of this transition for 1,22-docosanediol. It was the first time that this transition has been reported for 1,32-dotriacontanediol. These results were similar to those seen for *n*-alkanes. *n*-Alkanes H_3C–$(CH_2)_{n-2}$–CH_3, with $n = 9$–19 (odd *n* only) as well as all $n = 20$–43, have been shown to exhibit high-temperature phase transitions [30].

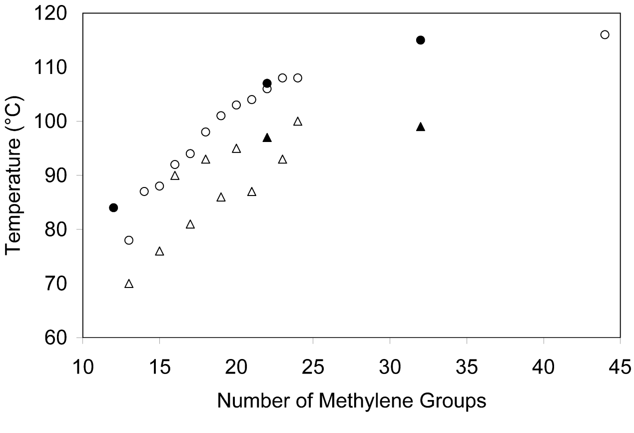

Fig. 2. Comparison of the melting and transition temperatures of the α,ω-diols. (●) and (○) represent data from this paper and literature Refs. [14,25], respectively; (○) and (△) represent melting and transition temperatures, respectively.

3.3. Polymer synthesis and characterization

The *m*,*n*-polyurethanes were all synthesized by step polyadditions in the melt (Scheme 3). Equimolar amounts of diol and diisocyanate were used. Lewis bases, such as tertiary

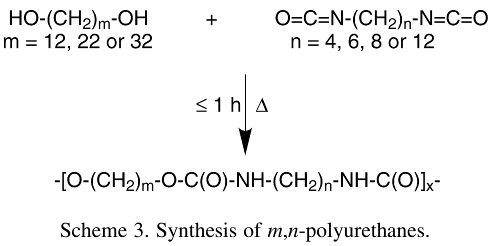

Scheme 3. Synthesis of *m*,*n*-polyurethanes.

Table 3
Polymerization conditions and resulting molecular weights for the *m*,*n*-polyurethanes

m,*n*-Polymer	Polymer temperature (°C)	Yield (%)	NMR solvent	$M_w \times 10^{-3}$	PDI	d*n*/d*c*[a] (ml g^{-1})
12,4	100	83	DMSO	4.7	1.6	−0.047
12,6	100	98	DMSO	3.2	2.0	−0.053
12,8	100	90	DMSO	11.4	1.9	−0.031
12,12	100	77	DMSO	19.5	2.2	−0.043
22,4	120	90	DMF	37.5	2.0	−0.039
22,6	120	97	DMSO	7.1	2.0	−0.058
22,8	120	81	DMF	13.8	2.0	−0.071
22,12	120	98	DMF	16.7	2.2	−0.063
32,4	130	59	DMF	20.3	2.1	−0.057
32,6	130	100	DMF	80.6	2.2	−0.069
32,8	130	78	DMF	63.8	2.2	−0.069
32,12	130	54	DMF	25.3	2.2	−0.039

[a] d*n*/d*c* determined using a wavelength of 690 nm in 1,2,4-trichlorobenzene at 135 °C.

amines, are often used to catalyze the isocyanate–alcohol reaction. However, care must be taken as some basic catalysts can promote trimerization [31] as well as the formation of cross-links [32]. In addition, the use of catalysts requires their removal from the resulting polymers. Since the emphasis of this research was not to make commercial polyurethanes where reactivity rates and molecular weights would be the critical criteria, but rather to synthesize model polymers whose purity and structure could be ensured, catalysts were not used. Isolated polymerization yields of 50–100% were obtained. Table 3 summarizes the polymerization conditions. The following *m*,*n*-polyurethanes were produced: 12,4; 12,6; 12,8; 12,12; 22,4; 22,6; 22,8; 22,12; 32,4; 32,6; 32,8; and 32,12. Except for the 12,6-polyurethane that had previously been synthesized by Saotome and Komoto in 1967 by a solution polyaddition in 60% yield [10], none of the other polyurethanes discussed in this paper had been previously synthesized.

Preliminary experiments proved the importance of the polymerization temperature. The temperature needed to be high enough to melt the diol, but too high a temperature resulted in known side reactions such as cross-linking via the formation of allophanates. These cross-links could be detected by GPC via a much higher than expected polydispersity index (PDI) (expected PDI = 2). Additionally, the hydroscopic diols had to be fully dried. Failure to do so resulted in the formation of known side products including amines, ureas, and cross-links via the formation of biurets. These side products could be detected using infrared spectroscopy.

The purity of all the polymers was carefully examined using IR, NMR, and GPC. These characterization methods indicated the absence of all known side products including cross-links. Some macrocyclics were expected since the polyurethanes were synthesized by a step-growth polymerization, but neither their presence nor concentration could be confirmed. Infrared and high temperature ^{1}H and ^{13}C NMR spectra were fully compatible with the expected structures. Very low amounts of the methylene groups alpha to hydroxyl and isocyanato end-groups were occasionally detected via ^{1}H NMR and infrared, respectively. The presence of these end-groups and their detection was expected based on the polymers' molecular weights as determined by GPC. The ^{13}C NMR spectra of the *m*,*n*-polyurethanes in DMSO-d_6 did not show a peak for the carbon of the methylene group alpha to the nitrogen of the carbamate ester. Presumably, the septet peak of the solvent at 39.7 ppm overlapped this peak. The peak was seen at 46.73–46.41 ppm when DMF-d_7 was used as the solvent. The absolute weight-average molecular weights of the polymers ranged from 3000–80 000 (Table 3). For all of the *m*,*n*-polyurethanes, the PDI was approximately 2 as is expected in a step growth polymerization.

3.4. Solubility

None of the crude *m*,*n*-polyurethanes dissolved in any common organic solvents at room temperature in an attempted range of concentration of 1–5 g l^{-1}. A number of solvents typically used for dissolving polyamides and polyurethanes were tried at elevated temperatures with varying success. *o*-Dichlorobenzene, a solvent often used to dissolve high-density polyethylene, was also tried. The results are summarized in Table 4. All the polymers dissolved in *m*-cresol, DMF, and *o*-dichlorobenzene. The temperatures needed to dissolve the samples in *m*-cresol were considerably lower than for the other solvents. However, upon cooling the polymers did not reprecipitate from the *m*-cresol, whereas they did reprecipitate from the other solvents. Therefore *m*-cresol could not be used as a solvent for growing single crystals. The solubility of the *m*,*n*-polyurethanes in *o*-dichlorobenzene increased with increasing alkane length as the polymers became more polyethylene-like. On the other hand, the solubility of the polymers decreased with increasing alkane length in more

Table 4
Solubility of the *m*,*n*-polyurethanes (reported in °C (see text); D and I represent degradation and insolubility (at temperatures up to the polymer's melting point) of the sample, respectively)

m,*n*-Polymer	Sulfuric acid	Formic acid	DMSO	*m*-Cresol	DMF	*o*-Dichlorobenzene
12,4	70	80	100	50	105	130
12,6	70	110	110	80	105	130
12,8	70	I	115	55	110	120
12,12	75	I	120	55	110	110
22,4	D	I	I	65	115	125
22,6	D	120	120	55	120	105
22,8	D	I	I	60	115	105
22,12	D	I	I	65	115	100
32,4	D	I	I	85	125	100
32,6	D	I	I	85	125	100
32,8	D	I	I	70	120	95
32,12	D	I	I	70	120	90

typical polyurethane solvents such as *m*-cresol and DMF. DMSO and formic acid, solvents typically used to dissolve polyamides and polyurethanes, were both able to dissolve the 12,*n*-polyurethanes. However, they were unable to dissolve the 22,*n*- and 32,*n*-polyurethanes with the exception of the lower molecular weight 22,6-polyurethane. Sulfuric acid was able to dissolve the 12,*n*-polyurethanes at only slightly elevated temperatures, but degraded the rest of the *m*,*n*-polyurethanes.

Table 5
Thermal properties of the *m*,*n*-polyurethanes

m,*n*-Polyurethane	Decomposition temperature[a] (°C)	Melting temperature[b] (°C)	Enthalpy (J g^{-1})
2,6[c]		166	39
4,6[c]		182	70
6,6[c]		171	70
8,6[c]		162	60
10,6[c]		161	56
12,4	292	167[d]	
12,6	303	160[d]	
12,8	303	150	110
12,12	307	141	89
22,4	286	158	71
22,6	292	146	89
22,8	301	144	90
22,12	306	137	93
32,4	295	150	123
32,6	291	143	112
32,8	316	139	104
32,12	309	135	117
HDPE[e]		145	295
LLDPE[f]		121–125	98–155

[a] Decomposition temperatures were taken at 5% weight loss using a scan rate of 10 K min^{-1}.

[b] Melting temperatures were taken as the peak of the melting endotherm during the second heating run using a scan rate of 10 K min^{-1}.

[c] See Ref. [32].

[d] These polymers had more than one endotherm (Fig. 4(a) and (b)), the melting points given were from the second endotherm.

[e] See Ref. [33].

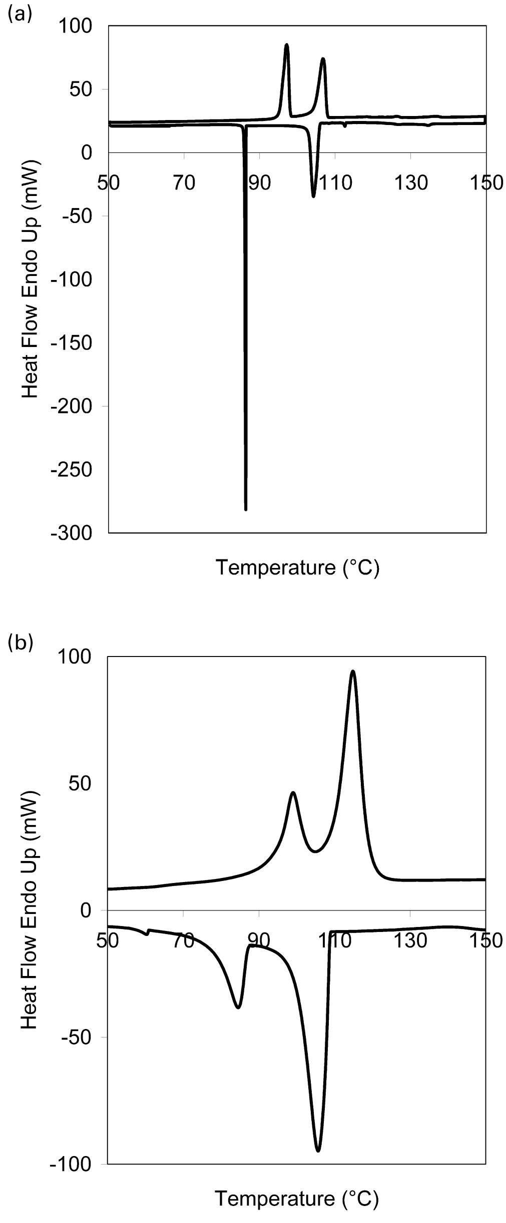

Fig. 3. DSC thermograms of the α,ω-diols. (a) 1,22-Diol and (b) 1,32-diol.

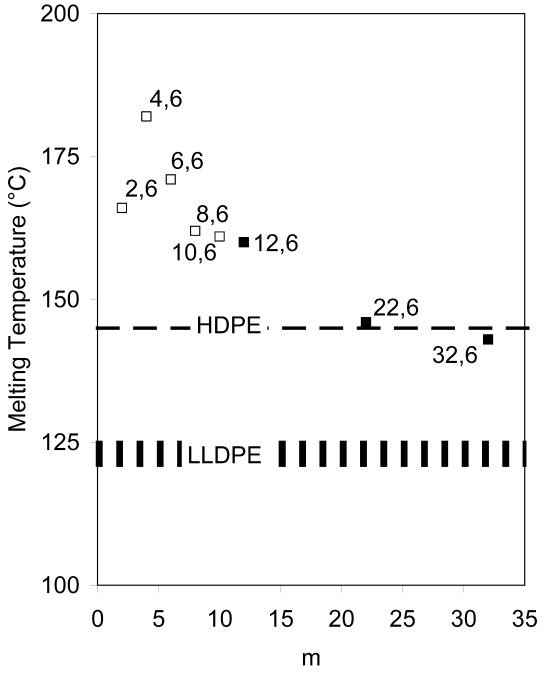

Fig. 4. Comparison of the melting points of *m*,6-polyurethanes. (■) and (□) represent data from this paper and literature Ref. [32], respectively.

3.5. Thermal analysis

The thermal properties of the *m*,*n*-polyurethanes, along with those of polyurethanes of higher hydrogen-bonding density [33] and both high-density [34] and linear low-density polyethylene [35], are summarized in Table 5. Decomposition temperatures of 200–300 °C were observed for all the polyurethanes. This agreed with the 220 °C or higher decomposition temperatures typically seen for aliphatic polyurethanes of higher hydrogen-bonding density [31].

As expected, the polymers exhibited decreasing melting points with increasing *m* or *n* (i.e. decreasing hydrogen-bonding density). As demonstrated by the *m*,6-polyurethanes in Fig. 4, increasing the length of the alkane segments resulted in decreased melting points. With long enough alkane segments, the melting points of the polyurethanes approached that of high-density polyethylene (145 °C) [34].

The measured heat of fusion increased with increasing *m* or *n* (i.e. decreasing hydrogen-bonding density). As with the melting temperature, the enthalpy appeared to be approaching that of high-density polyethylene (295 J g^{-1}) [34]. This last parameter, and the possible correlation with the structure of the polymer, has to be considered with prudence since there are other factors that could cause this increase including differences in percent crystallinity.

The melting and recrystallization behavior of the 12,4- and 12,6-polyurethanes differed from that of the other *m*,*n*-polyurethanes. Both polymers exhibited a melting endotherm, followed immediately by an exothermic peak, and then another endotherm (Fig. 5) upon heating. Upon cooling, both polyurethanes exhibited only one exothermic peak. Melting of the folded chains, followed by crystallization to the fully extended chain, and then melting of the extended chains could explain this behavior. The other

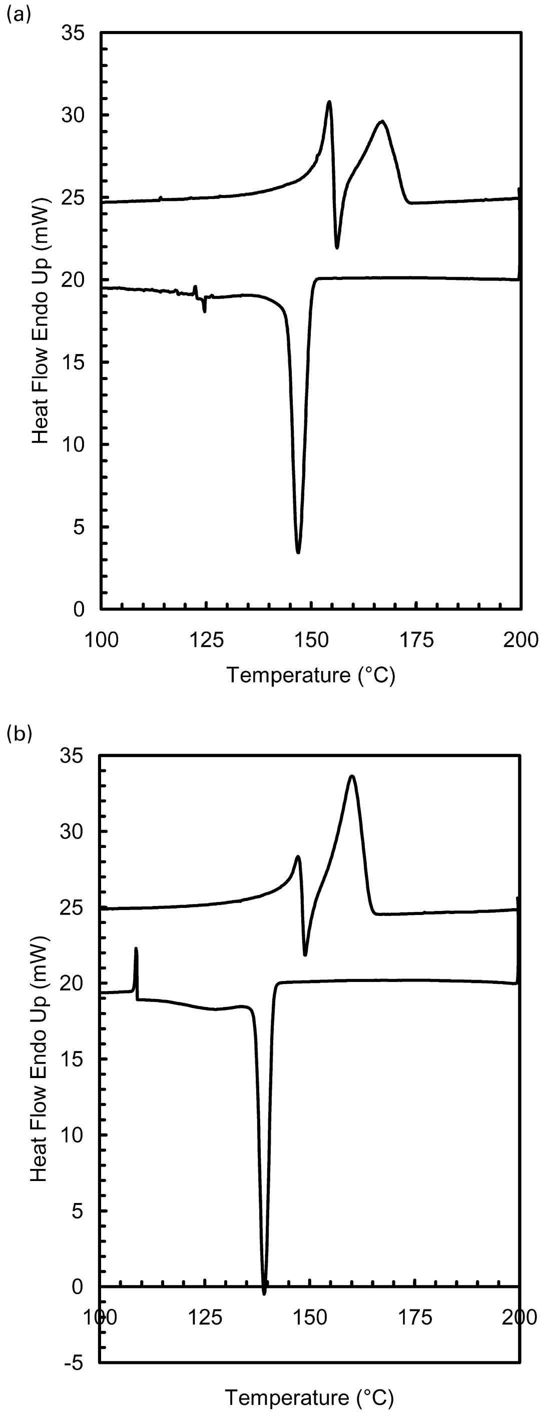

Fig. 5. DSC thermograms of (a) 12,4-polyurethane and (b) 12,6-polyurethane.

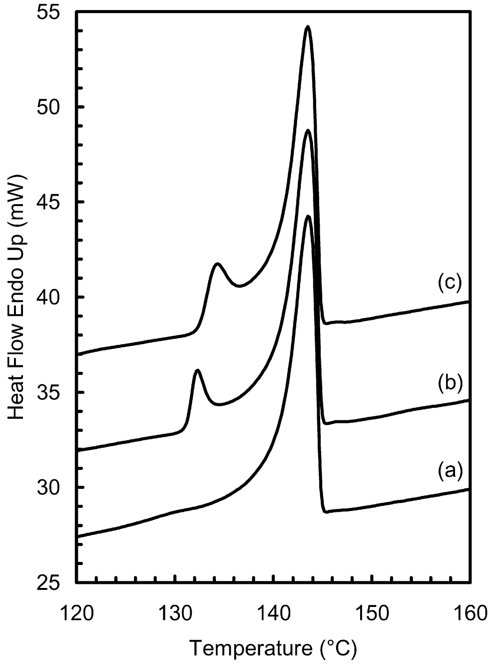

Fig. 6. Appearance of second, smaller endotherm upon annealing the 22,8-polyurethane. (a) Unannealed polymer; (b) polymer annealed for 1 h; and (c) polymer annealed for 15 h.

m,*n*-polyurethanes with their higher molecular weight exhibited only one melting endotherm.

The 22,*n*-polyurethanes were annealed at 10 °C below their melting points for both 1 and 15 h and then quenched to room temperature. The subsequent heating curves exhibited unexpected results. Rather than observing higher melting points as a result of an increase in the lamellar thickness, the polymers exhibited the same melting points as before, as well as a smaller endotherm at a lower melting point (Fig. 6). Upon cooling the annealed polymers, only one exothermic peak was exhibited. The melting points of these smaller peaks increased with increased annealing times (Table 6). These endotherms were most likely the result of some amorphous portions of the polymers organizing and crystallizing. The absence of chain thickening upon annealing suggested that these long chain, aliphatic *m*,*n*-polyurethanes could only increase their lamellar thickness in distinct steps similar to polyamides whose lamellae can thicken only by multiples of their repeat unit length [36].

Table 6
Melting points for annealed and unannealed 22,*n*-polyurethanes

22,*n*-Polyurethane	Unannealed (°C)	Annealed for 1 h (°C)	Annealed for 15 h (°C)
22,4	158	148 and 158	
22,6	146	137 and 146	
22,8	144	132 and 144	134 and 144
22,12	137	126 and 137	129 and 137

4. Conclusions

Several long chain, aliphatic diols were synthesized, and their thermal behavior was examined. As expected, their melting and decomposition temperatures increased with increasing alkane length. The existence of a solid–solid phase transition for 1,32-dotriacontanediol was reported for the first time. These long-chain diols were used to synthesize a series of novel *m*,*n*-polyurethanes with decreasing hydrogen-bonding density. Characterization of the polymers showed that the polyurethanes had low molecular weights and a PDI of approximately 2 as expected for polymers made by step growth polymerizations. Diluting the amount of carbamate esters by increasing the length of the aliphatic segments resulted in changing the physical and thermal characteristics from that typical of polyurethanes and polyamides to that of polyethylene. The crystal structure and crystallization of these polymers will be discussed in greater detail elsewhere [7,8].

Acknowledgements

This work is supported by NSF Material Research Science and Engineering Center (MRSEC) (NSF grant DMR-9809365). The use of MRSEC central experimental facilities, the Molecular Weight Characterization Laboratory (NSF Molecular Weight Determination grant DMR-9975762), and the Microanalytical Laboratory at the University of Massachusetts is acknowledged.

References

[1] Wunderlich B. Crystal structure, morphology, defects, vol. 1. New York: Academic, 1973.
[2] Dreyfuss P, Keller A. J Macromol Sci, Phys 1970;4:811.
[3] Saito Y, Nansai S, Kinoshita S. Polym J (Tokyo) 1972;3(2):113.
[4] Blackwell J, Gardner KH. Polymer 1979;20:13.
[5] Blackwell J, Ross M. J Polym Sci, Polym Lett Ed 1979;17:447.
[6] Saito Y, Hara K, Kinoshita S. Polym J (Tokyo) 1982;14(1):19.
[7] Heintz AM, McKiernan RL, Gido SP, Penelle J, Hsu SL. In press.
[8] McKiernan RL, Heintz AM, Hsu SL, Atkins EDT, Penelle J, Gido SP. Submitted for publication, 2002.
[9] McKiernan RL, Cardoen G, Boutevin B, Améduri B, Penelle J. Submitted for publication, 2002.
[10] Saotome K, Komoto H. J Polym Sci, Part A: Polym Chem 1967;5:119.
[11] Cho I, Lee K. Macromol Chem Phys 1997;198(3):861.
[12] Ehrenstein M, Dellsperger S, Kocher C, Stutzmann N, Weder C, Smith P. Polymer 2000;41:3531.
[13] Rusanova EE, Sebyakin YL, Volkova LV, Evstigneeva RP. Zh Org Khim (Engl Transl) 1984;20:279.
[14] Le Fevere de Ten Hove C, Jonas A, Penelle J. Polym Prepr (Am Chem Soc, Div Polym Chem) 1998;39:156.
[15] Ogawa Y, Nakamura N. Bull Chem Soc Jpn 1999;72(5):943.
[16] Hünig S, Buysch H. Chem Ber 1967;100(12):4017.
[17] Buchta E, Huhn C. Liebigs Ann Chem 1966;695:42.
[18] Grechishnikova IV, Johansson LB-Å, Molotkovsky JG. Chem Phys Lipids 1996;81(1):87.

[19] Furukawa A, Shoji H, Nakaya T, Imoto M. Makromol Chem 1987;188:265.

[20] Moss RA, Fujita T, Okumura Y. Langmuir 1991;7(11):2415.

[21] Kolattukudy PE, Agrawal VP. Lipids 1974;9(9):682.

[22] Austin PW, Seshadri TR, Sood MS. Indian J Chem 1969;7:43.

[23] Duhamel L. Ann Chim (Paris) 1963;8(13):315.

[24] Mazliak P. Phytochemistry 1962;1:79.

[25] Murray KE, Schoenfeld R. Aust J Chem 1955;8:432.

[26] Le Fevere de Ten Hove C. Controlling solid-state microstructure of semi-crystalline polymers through chemical design of chains: a study of model polyesters. PhD Thesis. Louvain-la-Neuve: Université Catholique de Louvain, 2001.

[27] Downing DT, Kranz ZH, Murray KE. Aust J Chem 1961;14:619.

[28] Lee K-S, Wagner G, Hsu SL. Polymer 1987;28:889.

[29] Kobayashi H, Nakamura N. Cryst Res Technol 1995;30:495.

[30] Broadhurst MG. J Res Natl Bur Stand, Sect A 1962;66:241.

[31] Sandler ST, Karo W, editors. Polyurethanes Polymer synthesis, vol. 1. San Diego: Academic, 1994. p. 232.

[32] Parodi F. In: Allen G, Bevington JC, editors. Isocyanate-derived polymers, Comprehensive polymer science, vol. 5. Oxford: Pergamon, 1989. p. 387.

[33] MacKnight WJ, Yang M, Kajiyama T. Polym Prepr (Am Chem Soc, Div Polym Chem) 1968;9:860.

[34] Mandelkern L, Alamo RG. Polyethylene, linear high-density. In: Mark JE, editor. Polymer data handbook. New York: Oxford University Press, 1999. p. 493.

[35] Prasad A. Polyethylene, linear low-density. In: Mark JE, editor. Polymer data handbook. New York: Oxford University Press, 1999. p. 508.

[36] Wunderlich B. Cyrstal nucleation, growth, annealing, vol. 2. New York: Academic, 1976.